Space Debris – Models and Risk Analysis

Heiner Klinkrad

Space Debris

Models and Risk Analysis

Springer

Published in association with
Praxis Publishing
Chichester, UK

PRAXIS

Dr. Heiner Klinkrad
European Space Agency
Darmstadt
Germany

Cover image shows a computer-generated snapshot of the observable population of space objects in 1997, based on orbit information provided by NASA.

SPRINGER–PRAXIS BOOKS IN ASTRONAUTICAL ENGINEERING
SUBJECT *ADVISORY EDITOR*: John Mason, M.Sc., B.Sc., Ph.D.

ISBN 3-540-25448-X Springer-Verlag Berlin Heidelberg New York

Springer is part of Springer-Science + Business Media (springeronline.com)

Bibliographic information published by Die Deutsche Bibliothek

Die Deutsche Bibliothek lists this publication in the Deutsche Nationalbibliografie; detailed bibliographic data are available from the Internet at http://dnb.ddb.de

Library of Congress Control Number: 2005936052

Printed in Germany

Cover design: Jim Wilkie
Completed in LaTeX: Heiner Klinkrad and Clare Martin
Cover image: © European Space Agency

Printed on acid-free paper

Table of Contents

Prolog

Most colleagues who enter the solemn halls of space flight use the main entrance, following the footsteps of generations of famous predecessors in their endeavor to conceive and realize new, ground-breaking space missions. Since I am dealing with residues of space flight, sometimes disrespectfully denoted as space junk, I approached these solemn halls from the alley way, through the back door. This was in 1978, when I got involved in the re-entry assessment of the reactor-equipped Cosmos 954 satellite after it spread its radioactive debris across Canada. At that time almost 6,000 trackable objects were on orbit, with more than 90% thereof space debris. Space debris are useless space objects including spent orbital stages, de-commissioned satellites, items released during nominal missions, and fragments from deliberate and unintentional on-orbit explosions, but also exotic relicts of space activities, such as protective gloves, or a screwdriver lost by an astronaut. The space debris population has steadily increased since the early 1960s. By the year 2005 more than 14,000 space objects of diameters larger than 5 to 10 cm could be tracked, of which no more than 5% were operational spacecraft. With these numbers in mind, and with 20 years of involvement in the field, I felt that it was time to write a book on space debris, which today represent the overwhelming majority of man-made objects in Earth orbits.

Several years elapsed between the first ideas for this book and its completion. Not just the space debris environment itself, but also the related research activities undergo a highly dynamic evolution. As a consequence, a book on space debris runs the risk of becoming inconsistent during the write-up process, and obsolete by the time of its publication. My intention was to minimize this risk by providing a consistent snapshot of the space debris situation around the year 2002, and by developing and documenting a theoretical basis with a hopefully better durability and longevity that the environment itself.

This book was written by a single author. In many chapters, however, the research contributions of several colleagues deserved more than a citation or acknowledgment. In such cases, they have been listed as contributing authors in the chapter headings.

This is not the first book dealing with space debris, nor will it be the last one. There could have been many different ways of selecting the material, of presenting it, and of citing relevant work. What you see here is a very personal, probably unintentionally biased presentation and view of the subject, based on information which I collected during 25 years of work for the European Space Agency, with 20 years thereof at the European Space Operations Center in Darmstadt, Germany. It was this environment, and the professional and personal links and information exchange with ESA colleagues, and with colleagues of the European and international space debris community, which made this book possible. Above all, I would like to acknowledge the role of Walter Flury, who has led ESA's space debris activities since the mid 1980s. His dedication and enthusiasm helped to advance space debris research in ESA and within Europe, and it helped to develop a European space debris expertise which today has reached an internationally recognized level.

The content of the book is largely focused on European activities, in particular on those which were performed under the lead, or with the participation of ESA. The views expressed in this text, however, are those of the author, and they may not necessarily reflect those of ESA. Inconsistent or erroneous information which may be contained in this text are the sole responsibility of the author.

The topics which are addressed in this book follow the outline of a graduate course on *Space Debris* which I have given in a curriculum for aeronautical engineers since 2001. I have tried to keep the volume and technical detail of the presented material at a level which allows this text book to be used for teaching purposes at graduate level. Worked problems, which would have been helpful for teaching applications, are not yet contained in this text. They are, however, foreseen for a later release.

I would like to thank the publishing staff at Praxis and Springer for their endurance, and for their constructive comments and guidance during the preparation of the manuscript, and during the final typesetting of this book. The typesetting was done in LaTeX, by means of an expert-designed LaTeX class-file which was provided by Clare Martin, one of the contributing authors. Apart from the contributing authors I would also like to acknowledge support, contributions, or editorial comments from Ludger Leushacke, Thomas Schildknecht, Frank Schäfer, Michael Oswald, Sebastian Stabroth, Gerhard Drolshagen, Michel Lambert, Markus Landgraf, Cristina Hernández, Íñigo Mascaraque, Santiago Llorente, Dorothea Danesy, and Tom Mohr. There are many more individuals to whom I am grateful, and who may not recognize themselves in the previous acknowledgments. My apologies to all of you.

Finally, and most of all, I would like to thank my wife Angelika for her patience and for her continuous support.

Heiner Klinkrad
Seeheim-Jugenheim, July 2005

1

Introduction

H. Klinkrad

We seem to exist in a hazardous time, driftn' along here through space; nobody knows just when we begun, or how far we've gone in the race.

Benjamin Franklin

1.1 HISTORY OF THE EVOLVING SPACE DEBRIS RESEARCH

On June 29, 1961, the US Transit-4A satellite was launched from Kennedy Space Center on a Thor-Ablestar rocket. The spacecraft was deployed into an orbit altitude between 881 km and 998 km, with an orbit inclination of 66.8°. Transit-4A was cataloged by the First Aerospace Control Squadron of the US Air Force as the 116th space object since the launch of Sputnik-1 on October 4, 1957. At 06:08:10 UTC on June 29, 77 minutes after the injection and separation of Transit-4A and two additional payloads, the Ablestar upper stage exploded, distributing its dry mass of 625 kg across at least 298 trackable fragments, of which nearly 200 were still on orbit 40 years later. This first on-orbit break-up event in space history increased the observable number of man-made space objects instantaneously by at least a factor 3.5 (Portree and Loftus, 1993). Since this date space debris has been the largest contributor to the observable space object population, with on-orbit explosions as its largest single source.

The terms *space debris* and *orbital debris* are often used as synonyms, with the following definition, as adopted by the Inter-Agency Space Debris Coordination Committee (IADC): "Space debris are all man made objects including fragments and elements thereof, in Earth orbit or re-entering the atmosphere, that are non functional" (anon., 2002a). According to this definition, 46.5% of the cataloged space objects prior the Ablestar explosion had already been space debris, for in-

stance in the form of spent upper stages and mission-related release objects (not counting decommissioned satellites).

With increasing launch and deployment activities, the space debris environment also started to take shape. In August 1964 the first geostationary satellite, Syncom-3, was deployed. Since then, more than 800 objects have been placed in or close to the geostationary orbit (GEO). Fourteen years after the Syncom-3 launch, in June 1978, the first spacecraft explosion occurred in GEO. In 1979 Luboš Perek presented a paper on "Outer Space Activities *versus* Outer Space", which was the first to recommend space debris mitigation measures, including the re-orbiting of GEO spacecraft into a disposal orbit at the end-of-life (Portree and Loftus, 1993). All his recommended measures are still applicable today.

The low-Earth orbit regime (LEO), kept being the main proving ground for new space technologies. It experienced the first intentional explosion in October 1965, when the Cosmos-50 reconnaissance satellite was blown up after a mission-critical failure. In October 1968 Cosmos-249 was used as the first anti-satellite weapon (ASAT), destroying the Cosmos-248 target in a commanded explosion during a rendezvous operation. The growing space debris population in the 1970s was suspected by some analysts to have its origin in a series of such ASAT tests. However, novel analysis techniques devised by John Gabbard, and applied to a subset of the NORAD[1.1] catalog by Donald Kessler, revealed that explosions of nine Delta second stages between May 1975 and January 1981 were the main contributors. They alone accounted for 27% of the LEO catalog by 1981 (Portree and Loftus, 1993). Once the cause of these explosions had been identified by the stage manufacturer, remedial action was taken, and no further break-ups of Delta second stages were recorded thereafter. This can be regarded as one of the first effectively implemented space debris mitigation measures.

In 1977 Donald Kessler and Burton Cour-Palais predicted that man-made orbital debris would soon pose a higher collision risk in the LEO regime than natural meteoroids. One year later, in 1978, the same authors published a paper on "Collision Frequency of Artificial Satellites: The Creation of a Debris Belt". They postulated that within a few decades on-orbit collisions could become the primary source of new space debris (Portree and Loftus, 1993). In 1990 Donald Kessler investigated the problem further in a publication on "Collisional Cascading: The Limits of Population Growth in Low-Earth Orbits", which describes the consequences of a self-sustained growth of the space debris population, initially triggered by collisions between intact objects and ultimately sustained by collisions between collision fragments (this was later known as the "Kessler Syndrome"). Such a cascading process, which cannot be stopped in its advanced stage, could render certain altitudes shells in the LEO region unsafe for a long time. Seven years after this publication, in July 1996, the first accidental collision between two cataloged objects was recorded, when the Cerise satellite was damaged by a fragment of an Ariane orbital stage which exploded in November 1986.

Following the Salyut-1 precursor mission in 1971, which paved the way for a

[1.1] North American Aerospace Defense Command

permanent presence of humans in space, there was at least one space habitat on orbit after 1973, when Salyut-2 and Skylab were launched. These early space stations were manned for limited time periods of up to several months. After 1989, when Salyut-7 and Mir were operational, there was an uninterrupted presence of humans in space. After the launch of Columbia in 1981, the US Space Shuttle program also contributed to this record, although with limited residence times per mission of less than 17 days. In late 1998 the first elements of the International Space Station (ISS) were launched and integrated in orbit. Since the end of 2001 the ISS has been permanently manned. Space debris has played an important role both in the design and operation of the ISS, and of the Space Shuttle. The ISS manned modules are protected by debris and meteoroid protection shields which can defeat impactors of up to 1 cm size. The shields are based on a multi-layer design principle proposed by Fred Whipple in 1947. As of the early 1980s such shields were optimized in laboratory impact tests with high-performance accelerators which can propel objects of 1 cm size to orbital speeds. The energy release of such impactors is equivalent to an exploding hand grenade.

After the Challenger accident in January 1986 a flight rule was established for Space Shuttle operations, which outlines a procedure for collision avoidance of trackable space objects. A similar procedure is in place today for the ISS. On the average, the Shuttle performs one avoidance maneuver for every 3 months on orbit, while the ISS performs one avoidance maneuver per year.

The adopted definition of *space debris* also includes re-entry objects, which are captured by the Earth atmosphere. In fact about 66% of all cataloged objects in space history have decayed, with most of these burning up due to aerothermal heating. Some objects, however, can pose a risk either by surviving to ground impact, or by releasing dangerous substances into the atmosphere. The first risk object re-entry was of the latter kind. In April 1964, following a launcher failure, the Transit 5BN-3 satellite re-entered above the Indian Ocean, dispersing 1 kg of plutonium from its SNAP-9A radio-thermal generator into the atmosphere. In January 1978, three months after its launch, the reactor-equipped Cosmos-954 satellite re-entered uncontrolled over Canada. It spread its reactor fragments with 30 kg of radioactive uranium along a swath of $\sim$1,000 km length. This incident resulted in the first application of the 1972 UN Liability Convention, with Canada claiming six million dollars compensation. The event also triggered the preparation of "UN Principles Relevant to the Use of Nuclear Power Sources in Space" (anon., 2002b). In February 1983 Cosmos-1402, also equipped with a reactor, re-entered over the South Atlantic, with no evident environmental consequences. Since then, there has been no re-entry of a risk object with nuclear material on board. There were, however, re-entry events which posed a risk due to their large mass, and due to the resulting risk from surviving debris to the population on ground. This was for instance the case for Skylab, with a mass of 74 tons, which re-entered over the Indian Ocean and Australia in July 1979, and for Salyut-7, with a mass of 40 tons, which re-entered over South America in February 1991.

This short historic overview of the evolving field of space debris research has touched upon problems and identified solutions for a wide range of technical dis-

ciplines, and it has also highlighted fine examples of collecting scientific evidence for suspected debris sources, and their long-term effect on the debris environment. It was just a handful of dedicated scientists and engineers who realized in the 1970s that there may be a space debris problem. These few individuals propagated the topic against all odds to today's level of recognition in the scientific world. The author hopes that the spotlight on their debris-related work triggered the reader's interest to learn more about the theoretical background of space debris.

1.2 GUIDANCE FOR READING THIS BOOK

The following text is organized in such a way that individual chapters are largely self-standing, with chapter-wise bibliographies and numbering conventions for equations, figures, tables, and footnotes. Items which are common to the whole text or to several chapters are compiled in annexes, and in lists of symbols, abbreviations, tables, and figures. Finally, there is a list of bibliographic references covering the entire text, followed by an index.

A novice in the field of space debris is recommended to read Chapters 2 to 6 in sequence. They explain how the present space debris environment can be characterized, based on measurement data, how it can be modeled, based on different sources, how its future can be forecast, based on assumed traffic models, and how it can be positively influenced, based on recommended mitigation measures. Here and there it can be helpful to side-step to the Annexes A to C for some elementary orbit mechanics, and for some background information on the Earth atmosphere and on the geopotential. Chapters 7 to 9 are ordered with some logic, but they can also be studied individually, in arbitrary sequence. They describe special aspects of risk assessment and risk prevention from the viewpoint of on-orbit shielding, collision avoidance, and re-entry risk management. Annex D, with model data of the Earth population, should be referenced for the latter issue. Chapter 10 concludes the technical part of this text. It gives a short overview of the natural meteoroid and meteorite collision flux and its associated risks for spacecraft and for the population on ground. Finally, in Chapter 11 an overview is provided of the relevance of space debris research and associated policy and standardization issues in an international context.

1.3 REFERENCES

anon. (2002a). *IADC Space Debris Mitigation Guidelines*. issue 1, rev. 1.

anon. (2002b). *United Nations Treaties and Principles on Outer Space*. United Nations publications, Vienna, Austria.

Portree, D. and Loftus, J. (1993). Orbital Debris and Near-Earth Environmental Management: A Chronology. Technical Report 1320, NASA Reference Publication.

2

The Current Space Debris Environment and its Sources

H. Klinkrad

2.1 LAUNCH HISTORY AND THE RESULTING ORBITAL ENVIRONMENT

The space environment of man-made intact and debris objects is a mirror image of almost half a century of space activities following the launch of Sputnik-1 on October 4, 1957. The objects which have since been released into space are the result of launch activities, with the deployment of payloads, upper stages which injected them into orbit, and associated mission-related objects, such as launch adapters, lens covers, clamp-bands, and yo-yo de-spin devices. Further items were released unintentionally, such as screwdrivers or protective gloves during extra-vehicular activities of astronauts, slag particles produced during solid rocket motor burns, cooling liquids released from Russian reconnaissance satellites, or degradation products resulting from crack formations and small particle impacts on the coatings of satellites and upper stage surfaces. The most important single source of space objects, however, is on-orbit explosions of spacecraft and rocket stages, sometimes more than 20 years after their launch.

In order to understand the environment produced by man-made objects on Earth orbits, it is helpful to establish a proven starting point by first looking at consolidated, quasi-deterministic information on large-size objects, which can be observed and characterized in terms of orbit, origin (association with a launch event), and object properties. The most comprehensive data set for this category of objects is the NASA Satellite Situation Report (SSR), together with the so-called Two-Line Element (TLE) catalog of the US Strategic Command (USSTRATCOM, formerly US Space Command USSPACECOM). Both of these are based on observation data and orbit determinations from the US Space Surveillance Network (SSN). Due to limitations in the sensitivities of the SSN radars and telescopes, the lower size threshold of objects which can be observed and correlated with the catalog is on the order of 10 cm in the low-Earth orbit (LEO) regime, and on the order

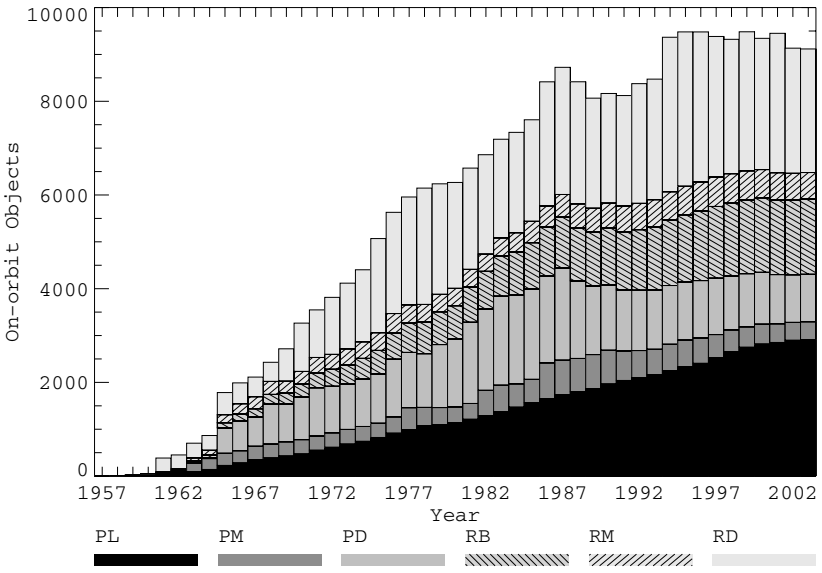

Fig. 2.1. Historic evolution of the number of trackable on-orbit catalog objects and their share between different source categories (PL = payloads, RB = rocket bodies, PM = PL mission-related objects, PD = PL debris, RM = RB mission-related objects, RD = RB debris).

of 1 m in the geostationary ring (GEO, see Fig. 6.16).

By January 2002 a total of 4,191 launches since 1957 had deployed 17,050 payloads, rocket bodies, and mission-related objects, which caused 27,044 detectable and trackable objects on Earth orbits. Of these 27,044 catalog objects, 18,051 had decayed into the atmosphere, leaving an on-orbit catalog population of 8,993. Fig. 2.1 shows the time evolution of the on-orbit catalog population according to source categories. As of 1962, a near-linear increase can be observed, at a rate of about 260 on-orbit objects per year. The total number of cataloged objects in the same time frame increased at a rate of about 710 per year. The linear rates are modulated with periods of 11 years, as a consequence of the solar cycle and its effect on air densities, which drive the orbit decay rates. With the end of the USSR around 1990/1991, the so far dominant launch nation, with peak contributions of about 80% to the overall launch rate, reduced its space activities significantly. The almost steady state annual launch rate of 110 ± 10 between 1965 and 1990 has dropped significantly since, to almost 50% of its original level. Since the years 2001/2002 it has seemed to settle at 60 launches per year. This decline in launch activities, a concurrent peak in solar activity, and a parallel reduction of on-orbit explosion rates due to post-mission passivation measures has resulted in an almost constant on-orbit catalog population close to 9,000 since 1994. Fig. 2.2 shows the historic evolution of the launch activities, and their share between major operators. Table 2.1 lists in more detail the originators of all 8,993 cataloged on-orbit objects for

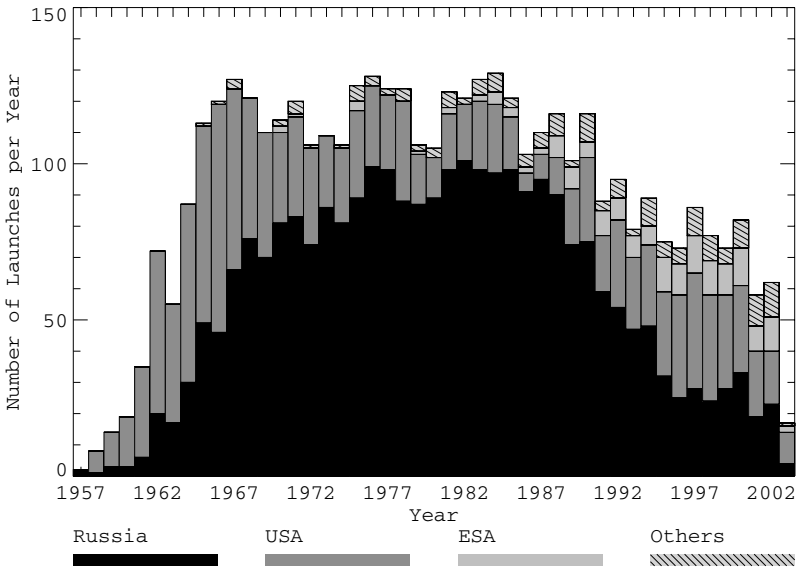

Fig. 2.2. Historic evolution of annual launch rates and their share between major operators (annual data for 2003 are incomplete).

January 1, 2002. When classified by object categories, 31.8% of these were payloads (∼6% thereof active satellites), 17.6% were spent rocket upper stages and boost motors, 10.5% were mission-related objects, and the remainder of ∼39.9% were debris, mainly from fragmentation events (28.4% caused by upper stages, and 11.5% caused by satellites). When classified according to orbit regime, 69.2% were in low-Earth orbits, at altitudes below 2,000 km, 9.3% were in the vicinity of the geostationary ring, 9.7% were on highly eccentric orbits (HEO), including the GEO transfer orbits (GTO), 3.9% were in medium Earth orbits (MEO), between LEO and GEO, and almost 7.8% were outside the GEO region. A small fraction, ∼150 objects, were injected into Earth escape orbits.

The spatial distribution of catalog orbits is shown in Fig. 2.3 as a global view from outside the GEO region. This image is a computer-generated snapshot of the instantaneous positions of all objects contained in the USSPACECOM catalog of 1997. The geostationary orbit region (GEO), with its distinct distribution signature, is clearly noticeable in this image. Objects on these orbits, close to the equator plane, at inclinations $i \approx 0°$, eccentricities $e \approx 0.0$, and altitudes $H \approx 35,876$ km move synchronously with the rotating Earth, at orbital periods of one sidereal day (23h 56m 04.09s). They are hence ideally suited for communications, broadcasting, and meteorological applications, which have a high commercial value. Consequently, the annual launch rates into GEO have attained a mean level of about 30 (∼25 of these payloads, and ∼5 of these upper stages), as shown in Fig. 2.5, with no significant effects due to the political changes around 1990. In contrast to the LEO region, there are no energy-dissipating perturbations effective in GEO

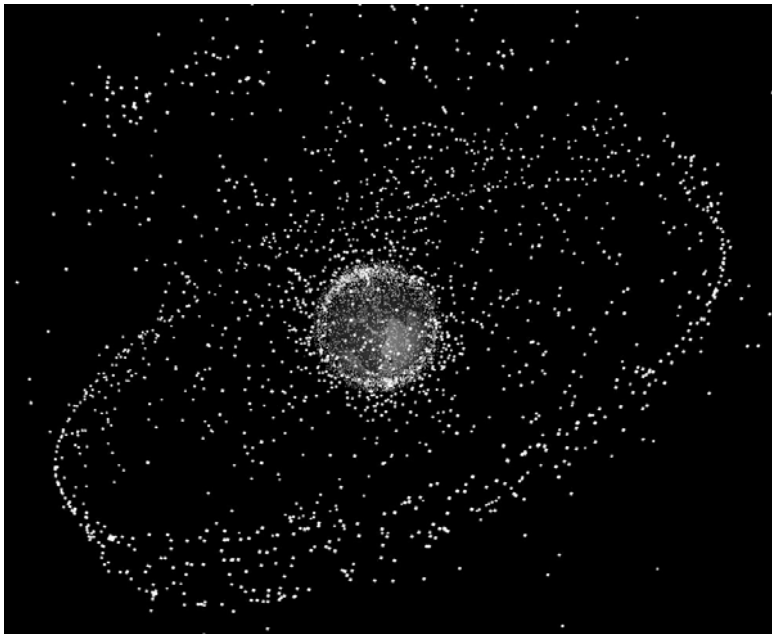

Fig. 2.3. Global snapshot of the catalog population in the year 1997 (source: ESA).

to remove objects from that altitude regime. Thus, the GEO catalog population is steadily increasing at a rate of about 30 per year. Fig. 2.4 indicates the growth history of trackable objects in GEO, and above the GEO ring (mainly in super-GEO "graveyard orbits"). In early 2002 the GEO ring was occupied by 485 payloads (active and non-active), and 108 rocket bodies or boost motors. 155 payloads and 60 rocket bodies were located on super-GEO orbits.

In later chapters, fragmentation processes (explosions and collisions) will be identified as dominating contributions to the evolution and stability of the future space debris environment. The determining parameters for the severity and frequency of fragmentation events are the masses and cross-sections of large orbital structures, predominantly of upper stages and spacecraft. Fig. 2.6 shows the time evolution of the on-orbit mass, which since the mid-1960s has increased by up to 1,500 tons per year, at a mean annual rate of about 110 tons, reaching a total of 5,100 tons by the year 2002. In the same time frame, the on-orbit cross-section, shown in Fig. 2.8 increased to 42,000 m^2, at a progressing rate over the last decade, with peak annual inputs of 3,600 m^2. This progression is due to the steady increase in the annually launched and deployed cross-section as indicated in Fig. 2.9, where, as for the annual launch masses in Fig. 2.7, the reduction of the USSR/Russian deployment activities was more than compensated by the USA.

The mass and cross-section deployment histories are strongly shaped by about 110 Shuttle launches, where each Shuttle had a dry mass of 78 tons, with a mean

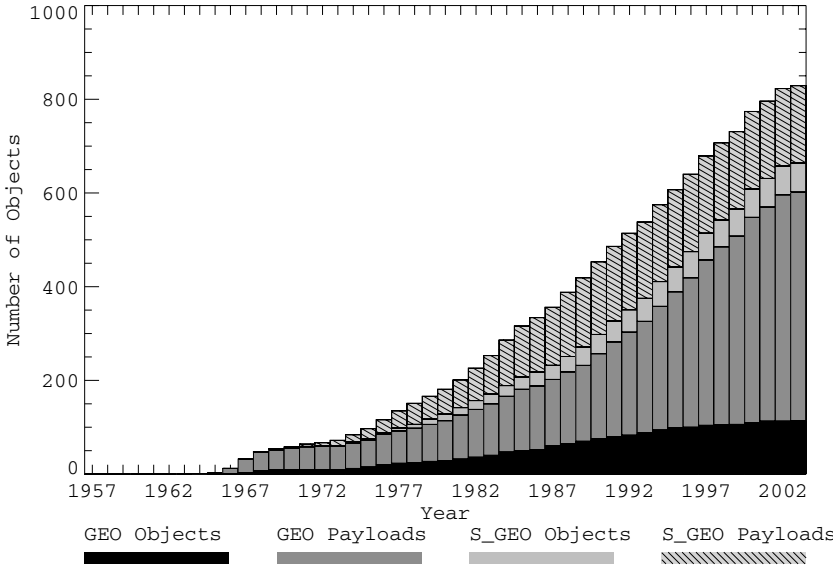

Fig. 2.4. Historic evolution of the number of trackable GEO and super-GEO (S_GEO) catalog objects and their share between payloads and upper stages.

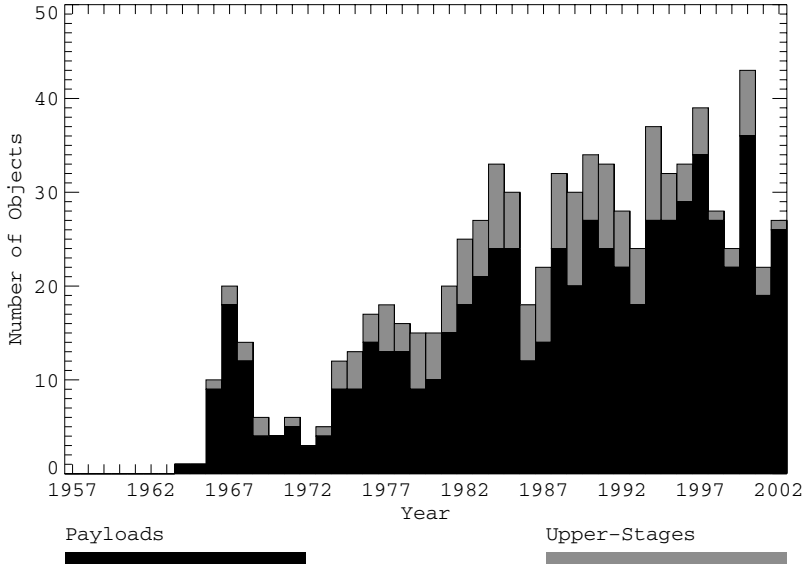

Fig. 2.5. Historic evolution of the annual launch rates into GEO and their share between payloads and upper stages (annual data for 2003 are incomplete).

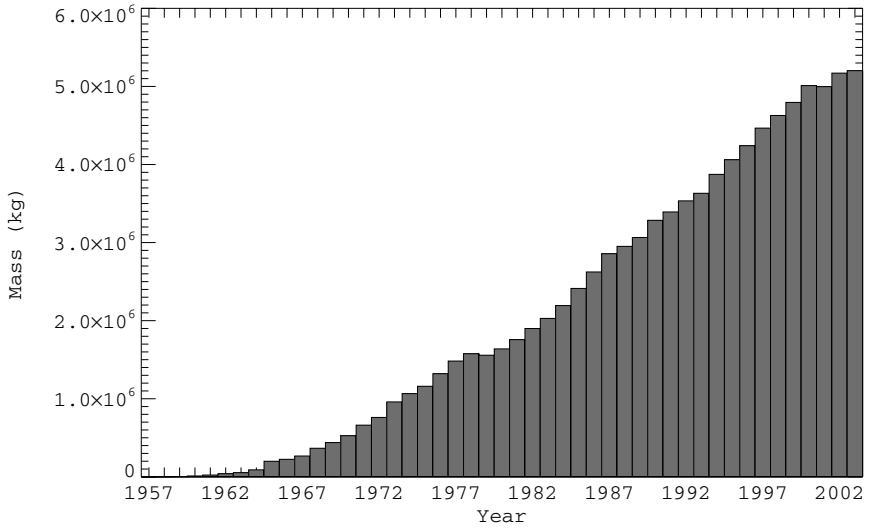

Fig. 2.6. Historic evolution of the on-orbit mass of catalog objects.

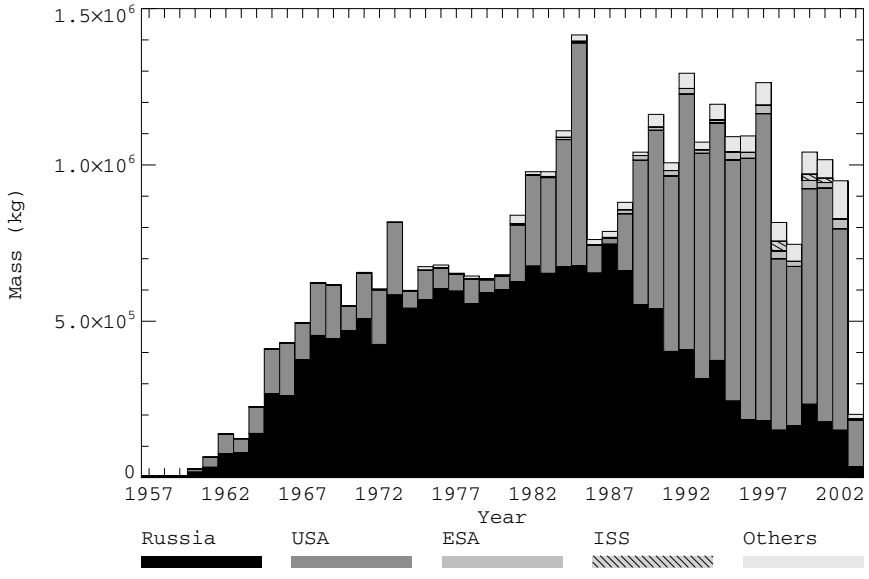

Fig. 2.7. Historic evolution of the annually launched mass of catalog objects and their share between major operators (annual data for 2003 are incomplete).

cross-section of 83 m^2, and a payload capacity to LEO of 24.4 tons. Moreover, several expandable launcher systems can deploy LEO payloads close to 20 tons

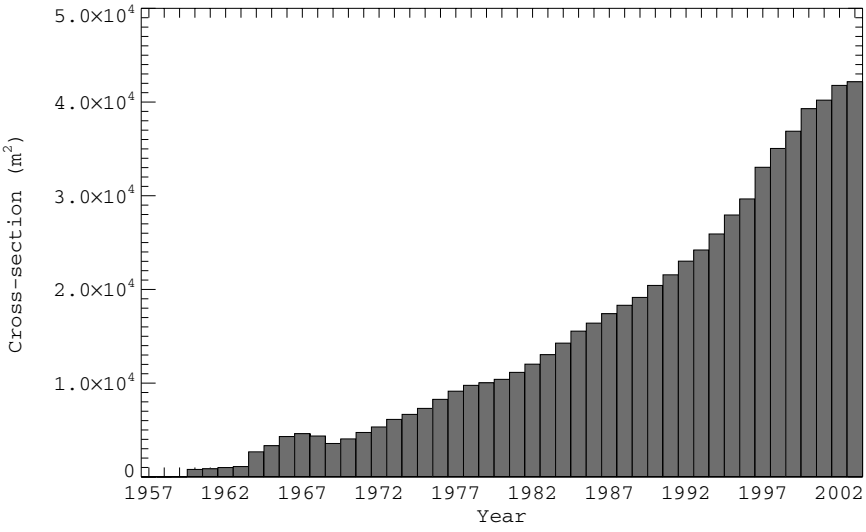

Fig. 2.8. Historic evolution of the on-orbit cross-section of catalog objects.

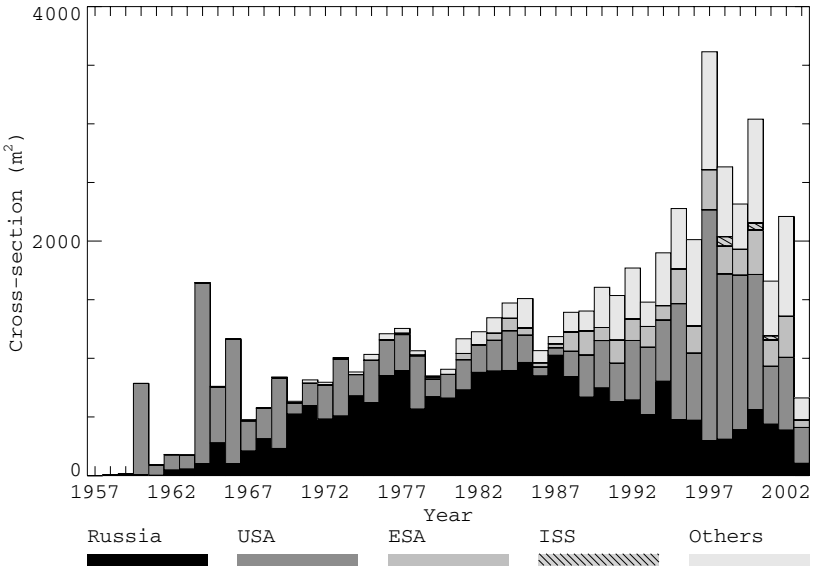

Fig. 2.9. Historic evolution of the annually launched cross-section of catalog objects and their share between major operators (annual data for 2003 are incomplete).

(Delta IV Heavy: 25.8 tons, Titan IV-B: 21.7 tons, Proton M: 21 tons, Atlas V 500: 20 tons, and Ariane 5: 18 tons). In this context, not just the launch capacity, but

also the launch frequency of different transport systems plays an important role. By the year 2002, there had been 1,099 launches by Soyuz vehicles, 422 by Cosmos, 301 by Molniya, 286 by the Atlas series, 280 by Delta, 269 by Proton, 248 by Tsyklon, 199 by Titan, 149 by Vostok, and 147 by different Ariane versions. Orbital stages of such launchers have typical cross-sections between 15 and 30 m^2, and the empty masses, particularly for LEO missions, can reach 9.0 tons for Zenith, 5.5 tons for CZ-2F, 4.8 tons for Tsyklon, 4.1 tons for Proton, 2.8 tons for Titan and Delta, and 2.3 tons for the most frequently used Soyuz and Molniya launchers. The distribution of the on-orbit mass and cross-section in 2002 is concentrated in regions which are of major scientific, commercial, and defense interest. With 45.0% the main mass fraction is in the LEO region, 28.8% is in the GEO vicinity, 6.4% is in MEO, 8.7% is in GTO and HEO, an 11.1% is located outside the GEO ring. The ranking is inverted when looking at the distribution of cross-sections, where 40.9% is concentrated near GEO, and 34.8% is within the LEO region. The reason for this characteristic distribution lies in the large appendages (solar arrays and antennas) of GEO satellites, leading to a lower mass-to-area ratio, and in the more compact design of LEO spacecraft to overcome airdrag, which entails higher mass-to-area ratios.

Table 2.1. Space object statistics as of January 1, 2002. 'payloads' = operational + non-operational spacecraft, and 'debris' = rocket bodies + mission-related objects + fragments (continued on next page).

Source/organization	Objects in orbit			Objects decayed		
	payloads	debris	total	payloads	debris	total
Argentina	4	0	4	2	0	2
Australia	7	0	7	2	0	2
Brazil	10	0	10	0	0	0
Canada	17	1	18	1	2	3
Chile	1	0	1	0	0	0
China	33	317	350	28	227	255
Czechoslovakia	4	0	4	1	0	1
Denmark	1	0	1	0	0	0
Egypt	2	0	2	0	0	0
EUMETSAT	3	3	6	0	0	0
ESA	33	281	314	5	541	546
ESRO	0	0	0	7	0	7
EUTELSAT	16	0	16	0	0	0
France	34	18	52	8	59	67
France/Germany	2	0	2	0	0	0
Germany	20	1	21	10	0	10
Hong Kong	3	0	3	0	0	0
India	21	7	28	8	10	18
Indonesia	10	0	10	1	0	1
INMARSAT	9	0	9	0	0	0

Table 2.1. Space object statistics as of January 1, 2002. 'payloads' = operational + non-operational spacecraft, and 'debris' = rocket bodies + mission related objects + fragments (continued from previous page).

Source/organization	Objects in orbit			Objects decayed		
	payloads	debris	total	payloads	debris	total
Space Station (ISS)	4	0	4	0	10	10
INTELSAT	56	0	56	2	0	2
Israel	3	0	3	3	3	6
Italy	12	2	14	7	0	7
Japan	73	48	121	14	103	117
Korea, Rep. of	7	1	8	0	0	0
Luxembourg	12	0	12	0	0	0
Malaysia	3	0	3	0	0	0
Mexico	6	0	6	0	0	0
Morocco	1	0	1	0	0	0
NATO	8	0	8	0	0	0
Netherlands	0	0	0	1	0	1
Norway	3	0	3	0	0	0
Pakistan	1	0	1	1	0	1
Philippines	2	0	2	0	0	0
Portugal	1	0	1	0	0	0
Saudi Arabia	9	0	9	0	0	0
Singapore	1	0	1	0	0	0
South Africa	1	0	1	0	0	0
Spain	6	0	6	0	0	0
Sweden	10	0	10	0	0	0
Taiwan	1	0	1	0	0	0
Thailand	4	0	4	0	0	0
Turkey	3	0	3	0	0	0
United Emirates	1	0	1	0	0	0
United Kingdom	23	1	24	9	1	10
USA	1,007	2,905	3,912	718	3,940	4,658
USSR	1,119	2,036	3,155	1,690	9,750	11,440
Russian Fed.	246	519	765	161	726	887
Column totals	2,853	6,140	8,993	2,679	15,372	18,051
Sum total						**27,044**

As a result of airdrag perturbations on LEO orbits and luni-solar perturbations on highly eccentric orbits (mostly in concert with airdrag), a large fraction of the catalog objects which were released into orbits have in the meantime decayed into the atmosphere. A smaller fraction has been intentionally de-orbited, or recovered by controlled re-entries. By the year 2002, out of the 27,044 objects cataloged since 1957, 18,051 had re-entered (66.7%). In the same time frame, a total mass of about 27,050 tons (84%), and a cumulative cross-section of about 85,000 m^2 (67%)

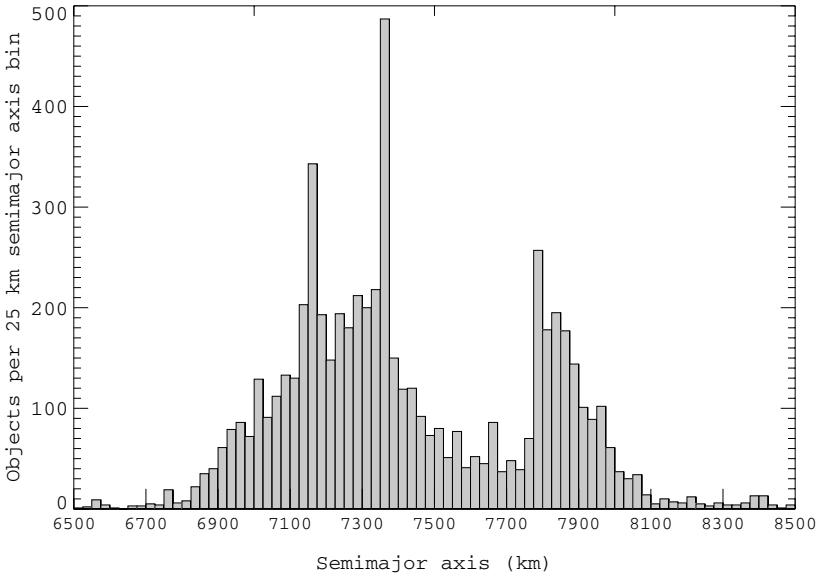

Fig. 2.10. Histogram of the distribution of LEO catalog objects with the semimajor axis of their orbit (class width: $\Delta a = 25$ km; status: June 2003).

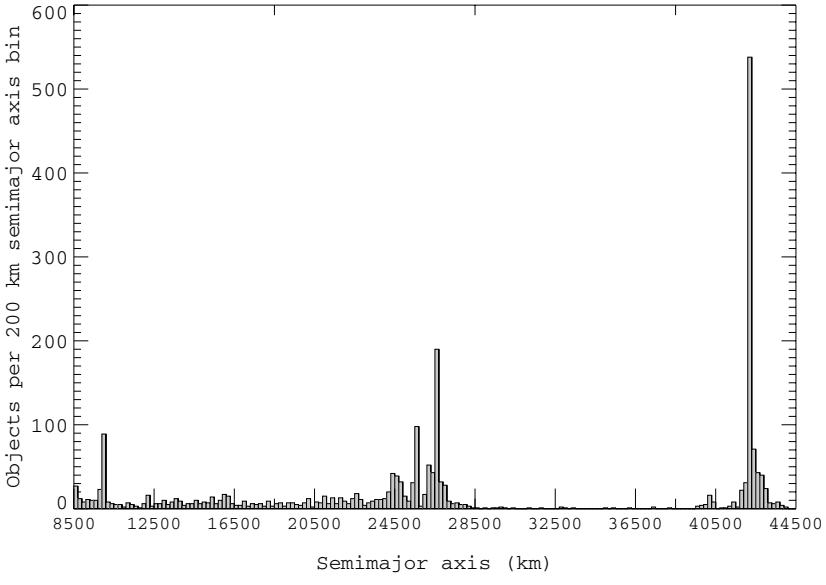

Fig. 2.11. Histogram of the distribution of super-LEO catalog objects with the semimajor axis of their orbit (class width: $\Delta a = 200$ km; status: June 2003).

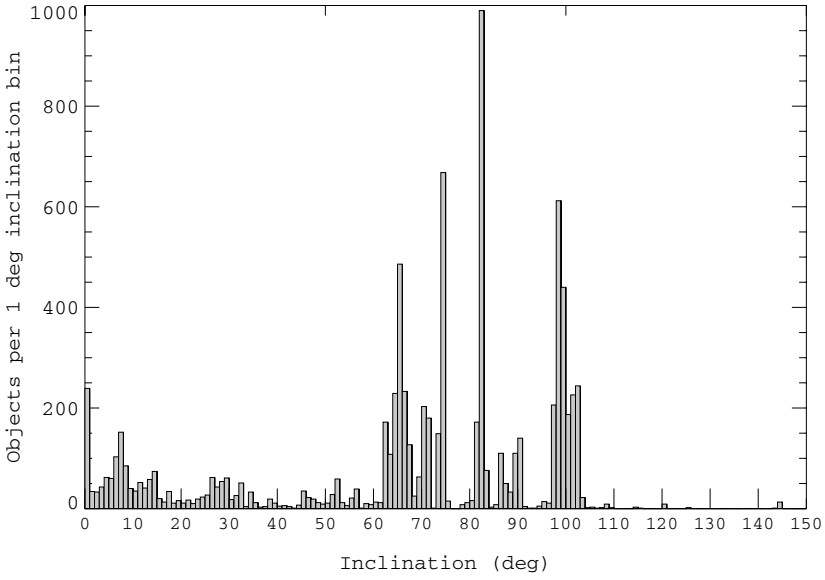

Fig. 2.12. Histogram of the distribution of catalog objects with the inclination of their orbit (class width: $\Delta i = 1°$; status: June 2003).

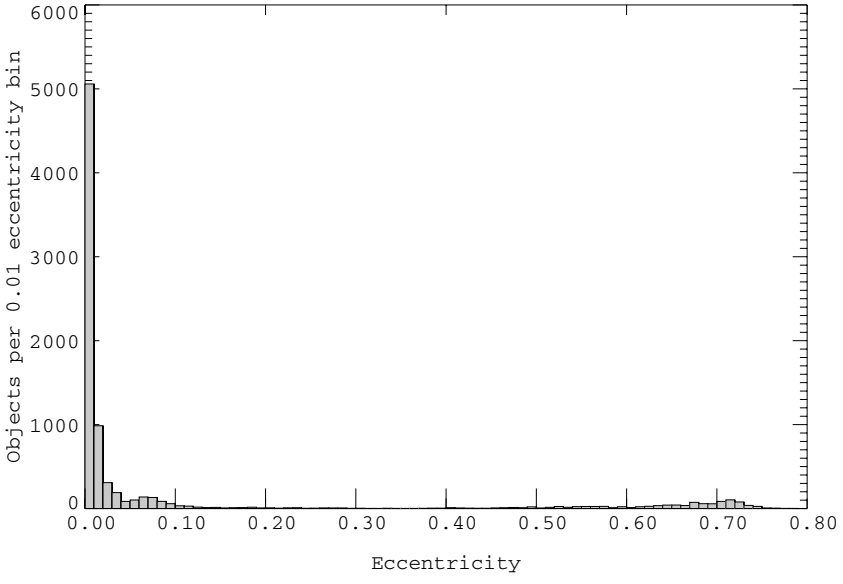

Fig. 2.13. Histogram of the distribution of catalog objects with the eccentricity of their orbit (class width: $\Delta e = 0.01$; status: June 2003).

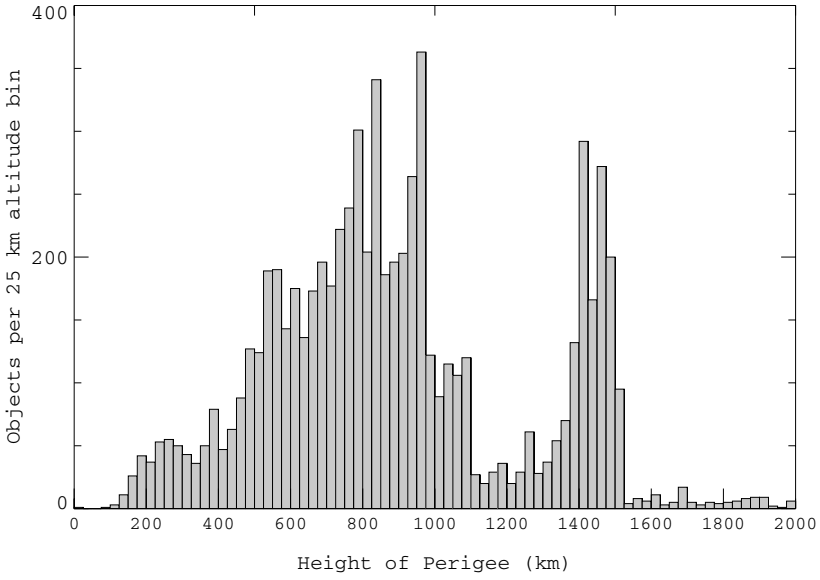

Fig. 2.14. Histogram of the perigee altitude distribution of LEO catalog objects (class width: $\Delta H_{pe} = 25$ km; status: June 2003).

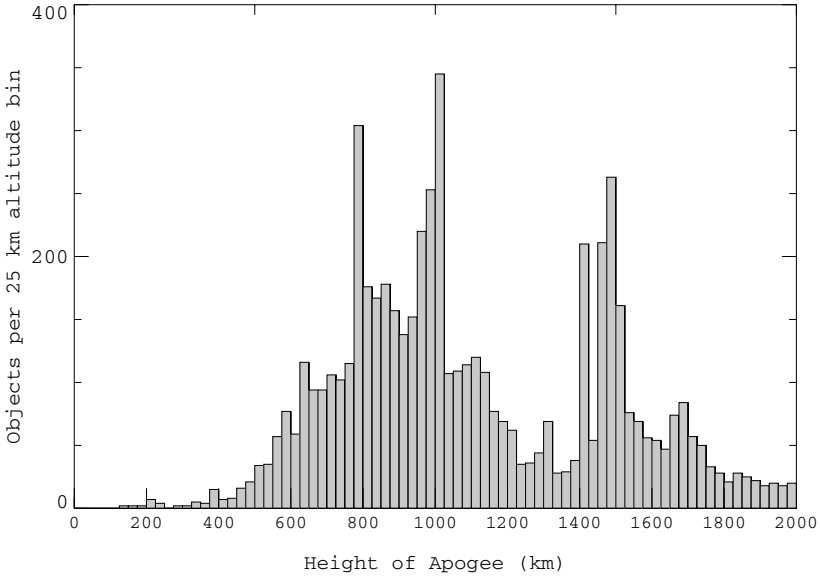

Fig. 2.15. Histogram of the apogee altitude distribution of LEO catalog objects (class width: $\Delta H_{ap} = 25$ km; status: June 2003).

decayed from orbit due to natural forces, or due to induced de-orbit maneuvers. This corresponds to a mean annual mass and cross-section loss-rate of on-orbit catalog objects of 800 tons and 2,100 m^2 during the past few decades.

So far, for the characterization of trackable catalog objects, their spatial distribution was only broadly classified according to orbital regimes (mainly LEO, MEO, GEO, GTO/HEO). A more detailed analysis must be based on the orbital element distributions within the catalog population. Such distributions identify preferred altitude shells, inclination bands, and orbital eccentricities of past space activities. Resulting clusters of preferred orbits form the origin of different classes of space debris which will be dealt with in the following chapters.

Fig. 2.13 shows the distribution of orbit eccentricities e for a catalog population in 2003. Clearly, the vast majority of the trackable objects reside on near circular orbits with $e \leq 0.01$ (54.5%), or moderately eccentric orbits of $0.01 < e \leq 0.1$ (32.0%). Another important contribution is from highly eccentric orbits of $0.6 < e \leq 0.8$ (8.0%), which include the GEO transfer orbits of typical eccentricities around 0.73, and Molniya orbits of semi-synchronous 12-hour periods, with eccentricities around 0.74. The large range of eccentricities $0.1 < e \leq 0.6$ contributes only 5.7%, and $0.8 < e \leq 1.0$ applies to only 0.1% of the catalog objects.

Fig. 2.10 (for the LEO regime) and Fig. 2.11 (for the super-LEO regime) show the distribution of the semimajor axes a of catalog orbits in 2003. Since the majority of orbits are near-circular, these histograms also give an indication of the distribution of mean altitudes $\overline{H} = a - a_e$, where $a_e = 6378.135$ km is the equatorial Earth radius. For the LEO regime, Fig. 2.14 and Fig. 2.15 confirm that the distribution of perigee altitudes $H_{pe} = a(1-e) - a_e$ and apogee altitudes $H_{ap} = a(1+e) - a_e$ closely resemble the profile in Fig. 2.10. Peak concentrations in LEO are at altitude shells near 800 km, 950 km, and 1,450 km due to preferred operational orbits of remote sensing, weather, and science missions. Local spikes in the distribution can to some extent be correlated with constellation deployments (Iridium at 780 km, OrbComm at 825 km, and GlobalStar at 1,415 km), but also with on-orbit fragmentation events. The asymmetries between the perigee and apogee distributions is mainly due to HEO and GTO orbits with perigees between 200 km and 600 km. In the super-LEO regime (Fig. 2.11) such eccentric orbits show peaks at $a \approx 26,560$ km ($\sim$12 h Molniya orbits) and 24,500 km ($\sim$10.5 h GTO orbits). Further contributions to medium Earth orbits are due to the navigation constellations GPS/Navstar ($\sim$12 h orbits at $a \approx 26,560$ km and $\overline{H} \approx 20,180$ km) and GLONASS ($\sim$11.25 h orbits at $a \approx 25,510$ km and $\overline{H} \approx 19,130$ km). The most densely populated altitude band above LEO is centered at the geostationary ring ($\sim$24 h orbits at $a \approx 42,164$ km and $\overline{H} \approx 35,786$ km), occupied by predominantly low eccentricity, low inclination trajectories, with close to 550 objects within a 200 km altitude shell. This compares with peak concentrations in LEO of almost 400 within a 25 km shell (with a corresponding mean distance between catalog objects of 2,500 km).

In contrast with the continuous distributions of semimajor axes and eccentricities (and hence of perigee and apogee altitudes), the histogram of inclinations, occupied by catalog objects in the year 2003 (Fig. 2.12), shows very distinct, narrow bands, with peak concentrations of up to 1,000 objects per 1° bin at $i \approx 82^\circ$.

Concentration maxima can be associated with special mission types, such as: Sun-synchronous orbits ($i = 100 \pm 5^\circ$), polar orbits ($i \approx 90^\circ$), navigation satellite orbits ($i \approx 55^\circ$ and 65°), orbits of critical inclination ($i \approx 63.4^\circ$, see Annex A.9), and near-geostationary orbits ($i < 15^\circ$). Further peaks are correlated with launch site latitudes, with injection azimuth constraints, or with the delivery of a maximum payload mass into orbit. Such maximum payload capacity is obtained by taking advantage of the Earth rotation via a due east launch. Launch sites which fulfill corresponding azimuth constraints are: Plesetsk (latitude of $\phi = 62.8^\circ$, ΔV gain of $210\,\mathrm{m/s^2}$), Baikonur ($\phi = 45.6^\circ$, ΔV gain of $328\,\mathrm{m/s^2}$), Tanegashima ($\phi = 30.4^\circ$, ΔV gain of $400\,\mathrm{m/s^2}$), Kennedy Space Center ($\phi = 28.5^\circ$, ΔV gain of $410\,\mathrm{m/s^2}$), Xichang ($\phi = 28.2^\circ$, ΔV gain of $408\,\mathrm{m/s^2}$), and Kourou ($\phi = 5.2^\circ$, ΔV gain of $463\,\mathrm{m/s^2}$). The latitude dependent gain in ΔV during the launch can increase the deliverable payload mass by up to 5%. Hence, launches optimized for payload mass criteria are eastward, into orbits with inclinations $i \approx \phi$, leading to concentration peaks at $i \approx 63^\circ$, 52°, 28.5°, and 7°. More often, however, mission objectives dominate injection conditions, and hence Plesetsk and Baikonur are frequently launching into north-easterly directions towards the 82° and 74° inclination band. High inclination orbits are also serviced by the Vandenberg launch site, which due to its launch azimuth constraints has a southward launch corridor.

A good survey of the cataloged space object population in terms of sources and distributions is provided by (anon., 1995), (anon., 2001), (Verger et al., 1997), and (Klinkrad et al., 2003). Most of the information compiled here to characterize the trackable space object environment was extracted from DISCOS, ESA's Database and Information System Characterizing Objects in Space (Hernández et al., 2001). This relational database, which covers the complete space history, contains mission data and orbit histories, mass and cross-section details, launch and decay information, and supporting data on launchers, launch sites, and associated launch statistics. Major portions of the DISCOS data originate from USSPACECOM (now USSTRATCOM). They are routinely provided through the official web interface of SpaceTrack.

2.2 HISTORIC ON-ORBIT BREAK-UP EVENTS

In Section 2.1 fragmentation debris was identified as the most important source of catalog objects, with a contribution of $\sim$39.9% to the trackable population. By January 2002, in total 175 on-orbit fragmentation events were inferred from the detection of new objects and from the correlation of their determined orbits with a common source. In many instances, not just the source object, but also the fragmentation cause could be reconstructed with some confidence. Out of the 175 events, 48 are believed to have been deliberate explosions or collisions (causing 2,244 cataloged fragments), 52 may be attributed to propulsion system explosions (causing 3,558 cataloged fragments), 7 could be associated with electrical system failures (mainly battery explosions, causing 618 cataloged fragments), 10 may have been

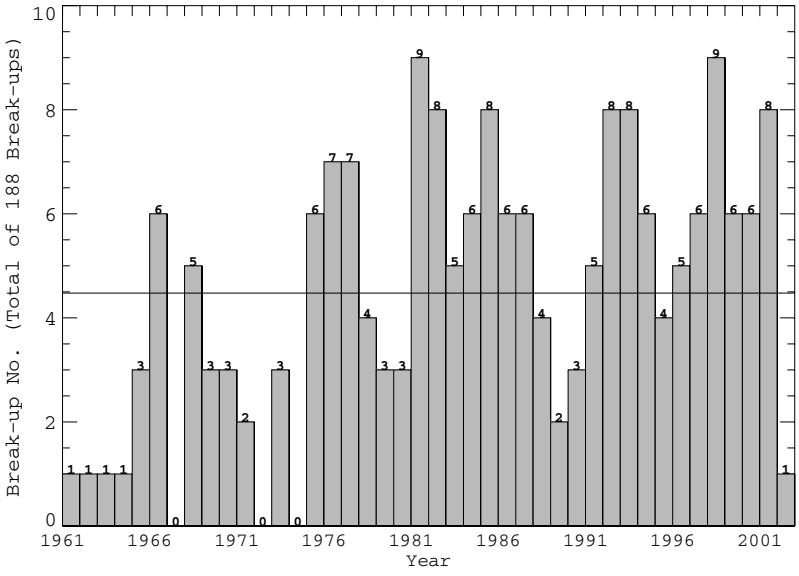

Fig. 2.16. Histogram of the annual count of on-orbit fragmentation events through January, 2002.

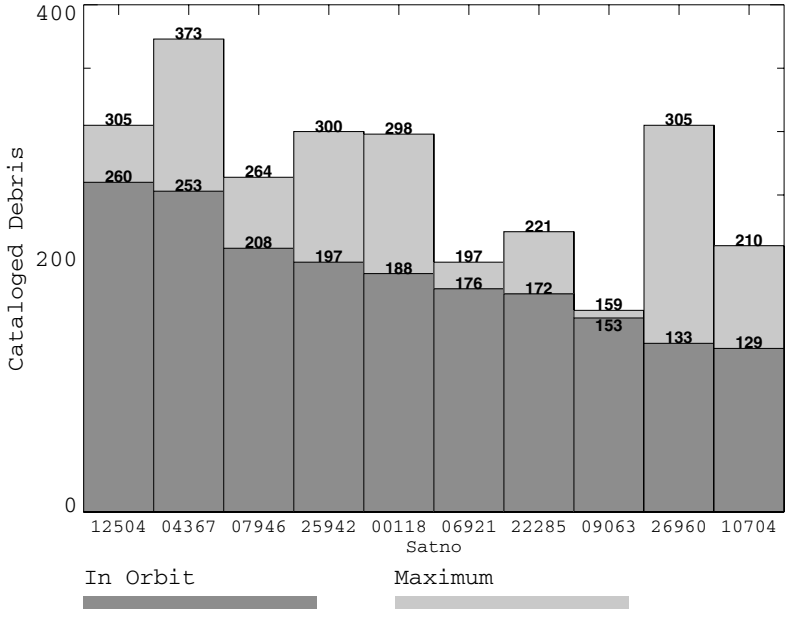

Fig. 2.17. Top ranking fragmentation events as of January 1, 2002, sorted by on-orbit catalog objects.

caused by aerodynamic forces, and at least one event was an accidental collision. The causes of 57 further break-up events could not be identified. With the exception of two GEO explosion events (an Ekran-2 satellite on June 22, 1978, and a Titan III-C Transtage on February 8, 1994), all known fragmentations occurred on orbits passing through altitudes below 2,000 km, with ∼80% of the orbits within LEO, and ∼17% on HEO and GTO.

The first unintentional collision in space history occurred between the French Cerise satellite (95-033B) and an Ariane-1 H-10 upper stage explosion fragment (86-019F), on July 24, 1996, at 09:48 UTC. The H-10 upper stage had previously delivered SPOT-1 into orbit on February 22, 1986, and exploded 9 months later, on November 13, 1986, causing one of the most severe fragment clouds in space history, with a total of 488 catalog entries (33 thereof still on orbit by January 2002, as shown in Table 2.2). Apart from this unintentional event, there were at least two deliberate collisions, both of them in context with SDI experiments (Strategic Defense Initiative). On September 13, 1985, Solwind P78-1 was destroyed by an anti-satellite (ASAT) missile, which was launched from a fighter aircraft, and intercepted the spacecraft during an ascending pass along the Californian coastline, on its 97.6° inclined orbit, at an altitude of about 530 km. The test scenario was selected such that the fresh fragment cloud could be observed by the SSN sensors in Alaska, and such that the orbital lifetime of the collision fragments was limited (Table 2.2 shows that only 2 out of 285 cataloged fragments were still on orbit in January 2002). Another intentional collision was brought about on September 5, 1986, between the USA-19 spacecraft and the Delta upper stage which previously injected it into orbit. The number of cataloged fragments in this case was only 13. Non-destructive collisions, for instance between a Progress cargo spacecraft and the Mir space station, are not included in the count of collision events. Fig. 2.16 indicates the annual break-up counts, which reached peak rates of 9 per year in 1981 and 1998, and a mean annual rate of about 4.5. Out of 175 events in total, there were 172 explosions or aerodynamic break-ups, and only 3 collisions.

Table 2.2 provides a summary of the top-ranking fragmentation events up to a cut-off date of January 1, 2002, sorted by maximum count of cataloged fragments on-orbit. Fig. 2.17 shows a corresponding histogram of the 10 most severe events, ranked by the number of on-orbit fragments for that date. The majority of the break-up events occurred within a few years after orbit injection, as indicated by the cumulation along a straight line in the plot of launch epoch versus fragmentation epoch in Fig. 2.18. In some cases, however, particularly upper stages exploded with a delay of more than a decade (the Titan III-C Transtage 1967-066G exploded 22 years after launch, and the Vostok stage 1964-006D exploded 33 years after launch). Fig. 2.18 also indicates than many fragmentations in recent years were caused by objects which were launched in the 1980s. Hence, end-of-life passivation measures (the release of latent on-board energies at mission termination), which have become common practice for many launch systems over the past decade, seem to prove their effectiveness.

Table 2.2. The most severe on-orbit fragmentation events as of reference epoch t_{ref} = 01 Jan 2002, sorted by the maximum number of cataloged debris. (∗) The number of correlated, on-orbit fragments of the PSLV upper stage fragmentation increased to 303 within one month after the reference epoch.

Catalog number	International designator	Source object name and type	Break-up date	Debris count max./t_{ref}	H_{pe}/H_{ap} [km]/[km]	i [°]	Assessed cause
23106	1994-029B	Pegasus R/B	03-Jun-1996	703/76	586/821	82.0	Unknown
16615	1986-019C	Ariane-1 R/B	13-Nov-1986	488/33	803/833	98.7	Unknown
1640	1965-082B	Titan III-C Transtage R/B	15-Oct-1965	470/41	658/761	32.0	Propulsion
4367	1970-025C	Thor Agena D R/B	17-Oct-1970	373/253	1063/1087	99.9	Unknown
12504	1981-053A	Cosmos 1275 S/C	24-Jul-1981	305/260	960/1014	83.0	Electrical
26960	2001-049D	PSLV R/B	19-Dec-2001	303/133 (∗)	549/674	97.9	Propulsion
25942	1999-057C	CZ-4B stage 3 R/B	11-Mar-2000	300/197	727/745	98.5	Propulsion
118	1961-015C	Thor Ablestar R/B	29-Jun-1961	298/188	882/997	66.8	Propulsion
11278	1979-017A	Solwind P-78 ASAT test	13-Sep-1985	285/2	515/546	97.6	Deliberate
7946	1975-052B	Delta-1 R/B	01-May-1991	264/208	1093/1102	99.6	Propulsion
4159	1969-82AB	Thor Agena D R/B	04-Oct-1969	259/75	917/1091	70.0	Unknown
9046	1976-072A	Cosmos 844 S/C	25-Jul-1976	248/0	172/353	67.0	Unknown
6127	1972-058B	Delta-1 R/B	22-May-1975	226/35	633/909	98.3	Propulsion
22285	1992-093B	Zenit-2 R/B	26-Dec-1992	221/172	847/854	71.0	Propulsion
10704	1978-026C	Delta-1 R/B	27-Jan-1981	210/129	879/912	98.9	Propulsion
7616	1975-004B	Delta-1 R/B	19-Jun-1976	206/33	734/918	97.8	Propulsion
26040	1999-072A	Cosmos 2367 S/C	21-Nov-2001	200/17	405/417	65.0	Accidental
6921	1973-086B	Delta-1 R/B	28-Dec-1973	197/176	1494/1516	102.1	Propulsion
6432	1973-021A	Cosmos 554 S/C	06-May-1973	195/0	147/349	72.8	Deliberate
17297	1987-004A	Cosmos 1813 S/C	29-Jan-1987	194/0	346/405	72.8	Deliberate
10144	1977-065B	Delta-1 R/B	14-Jul-1977	169/65	537/2036	29.1	Propulsion
1093	1965-012A	Cosmos 57 S/C	22-Feb-1965	167/0	169/419	64.8	Deliberate
9063	1976-077B	Delta-1 R/B	24-Dec-1977	159/153	1502/1522	102.0	Propulsion
14064	1983-044A	Cosmos 1461 S/C	11-Mar-1985	158/3	584/883	65.0	Unknown